Anisotropic materials in OLEDs for high outcoupling efficiency

Michiel Koen Callens,[1,*] Daisuke Yokoyama,[2] and Kristiaan Neyts[1]

[1]*ELIS Department, Ghent University, Sint-Pietersnieuwstraat 41, B-9000, Ghent, Belgium*
[2]*Department of Organic Device Engineering and Research Center for Organic Electronics (ROEL), Yamagata University, 4-3-16 Jonan, Yonezawa, Yamagata 992-8510, Japan*
**michiel.callens@elis.ugent.be*

Abstract: We present the results of an optical study in which we evaluate the effect of anisotropic electron transport layers (ETL) and anisotropic hole transport layers (HTL) on the outcoupling efficiency of bottom emitting organic light emitting diodes (OLEDs). We demonstrate that optical anisotropy can have a profound influence on the outcoupling efficiency and introduce a number of design rules which ensure that light extraction is enhanced by anisotropic layers.

OCIS codes: (160.4890) Organic materials; (230.3670) Light-emitting diodes; (260.1440) Birefringence; (160.1190) Anisotropic optical materials; (240.0310) Thin films.

References and links

1. C. Adachi, M. A. Baldo, M. E. Thompson, and S. R. Forrest, "Nearly 100% internal phosphorescence efficiency in an organic light-emitting device," J. Appl. Phys. **90**(10), 5048 (2001).
2. K. A. Neyts, "Simulation of light emission from thin-film microcavities," J. Opt. Soc. Am. A **15**(4), 962–971 (1998).
3. S. Reineke, F. Lindner, G. Schwartz, N. Seidler, K. Walzer, B. Lüssem, and K. Leo, "White organic light-emitting diodes with fluorescent tube efficiency," Nature **459**(7244), 234–238 (2009).
4. W. H. Koo, S. M. Jeong, F. Araoka, K. Ishikawa, S. Nishimura, T. Toyooka, and H. Takezoe, "Light extraction from organic light-emitting diodes enhanced by spontaneously formed buckles," Nat. Photonics **4**(4), 222–226 (2010).
5. M. K. Callens, H. Marsman, L. Penninck, P. Peeters, H. de Groot, J. M. ter Meulen, and K. Neyts, "RCWA and FDTD modeling of light emission from internally structured OLEDs," Opt. Express **22**(S3 Suppl 3), A589–A600 (2014).
6. C. Fuchs, T. Schwab, T. Roch, S. Eckardt, A. Lasagni, S. Hofmann, B. Lüssem, L. Müller-Meskamp, K. Leo, M. C. Gather, and R. Scholz, "Quantitative allocation of Bragg scattering effects in highly efficient OLEDs fabricated on periodically corrugated substrates," Opt. Express **21**(14), 16319–16330 (2013).
7. K. Saxena, V. K. Jain, and D. S. Mehta, "A review on the light extraction techniques in organic electroluminescent devices," Opt. Mater. **32**(1), 221–233 (2009).
8. W. Brütting, J. Frischeisen, T. D. Schmidt, B. J. Scholz, and C. Mayr, "Device efficiency of organic light-emitting diodes: progress by improved light outcoupling," Phys. Status Solidi **210**(1), 44–65 (2013).
9. D. Yokoyama, "Molecular orientation in small-molecule organic light-emitting diodes," J. Mater. Chem. **21**(48), 19187 (2011).
10. D. Yokoyama and C. Adachi, "In situ real-time spectroscopic ellipsometry measurement for the investigation of molecular orientation in organic amorphous multilayer structures," J. Appl. Phys. **107**(12), 123512 (2010).
11. S. Y. Kim, W. I. Jeong, C. Mayr, Y. S. Park, K. H. Kim, J. H. Lee, C. K. Moon, W. Brütting, and J. J. Kim, "Organic light-emitting diodes with 30% external quantum efficiency based on a horizontally oriented emitter," Adv. Funct. Mater. **23**(31), 3896–3900 (2013).
12. K. H. Kim, S. Lee, C. K. Moon, S. Y. Kim, Y. S. Park, J. H. Lee, J. Woo Lee, J. Huh, Y. You, and J. J. Kim, "Phosphorescent dye-based supramolecules for high-efficiency organic light-emitting diodes," Nat. Commun. **5**, 4769 (2014).
13. D. Yokoyama, K. Nakayama, T. Otani, and J. Kido, "Wide-range refractive index control of organic semiconductor films toward advanced optical design of organic optoelectronic devices," Adv. Mater. **24**(47), 6368–6373 (2012).
14. D. Yokoyama, H. Sasabe, Y. Furukawa, C. Adachi, and J. Kido, "Molecular stacking induced by intermolecular C-H · · ·N hydrogen bonds leading to high carrier mobility in vacuum-deposited organic films," Adv. Funct. Mater. **21**(8), 1375–1382 (2011).

#241444 Received 21 May 2015; revised 3 Jul 2015; accepted 17 Jul 2015; published 4 Aug 2015

15. C.-K. Moon, S.-Y. Kim, J.-H. Lee, and J.-J. Kim, "Luminescence from oriented emitting dipoles in a birefringent medium," Opt. Express **23**(7), A279–A291 (2015).
16. L. Penninck, F. Steinbacher, R. Krause, and K. Neyts, "Determining emissive dipole orientation in organic light emitting devices by decay time measurement," Org. Electron. **13**(12), 3079–3084 (2012).
17. E. M. Purcell, "Spontaneous emission probabilities at radio frequencies," Phys. Rev. **69**, 681 (1946).
18. K. Walzer, B. Maennig, M. Pfeiffer, and K. Leo, "Highly efficient organic devices based on electrically doped transport layers," Chem. Rev. **107**(4), 1233–1271 (2007).

1. Introduction

Organic light emitting diodes (OLEDs) are luminescent devices consisting of a stack of thin organic layers. Each of these layers has a specific function and, when an appropriate combination of layers and emitters is used, one can make these devices generate light with nearly 100% internal efficiency [1]. Even though light can be generated with such high efficiencies, only a relatively small portion can be extracted from the structure. Due to total internal reflection (TIR) at surfaces of media with a lower refractive index and coupling to plasmonic modes, a large portion of the light remains trapped inside the stack and is eventually absorbed [2].

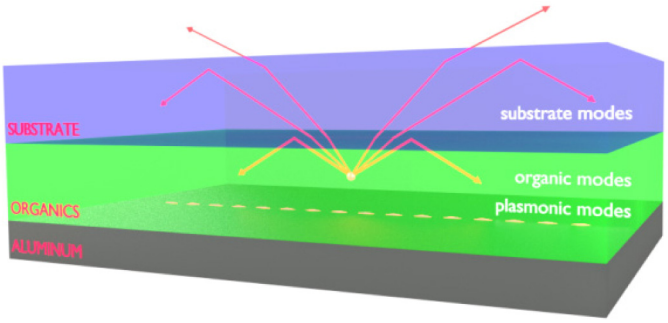

Fig. 1. Simplified schematic drawing of optical loss mechanisms in an OLED stack. There is coupling to plasmonic modes as well as coupling to organic and substrate modes. Radiation coupled to these modes is eventually absorbed and never escapes the device. In a standard device only around 20–30% of the light escapes the OLED device. Layer thicknesses are not to scale.

In a traditional OLED, the percentage of light that manages to escape the structure and is considered useful is usually limited to around 20–30% as illustrated in Fig. 1. Because losses are so high, there is a lot of potential for improvement. A plurality of solutions have been proposed to increase OLED efficiency, such as high-index substrates [3], grating-assisted outcoupling [4–6] and many others [7]. We refer to the work of Brütting et al. [8] for an overview. In recent developments, Yokoyama et al. [9,10] showed that many amorphous organic materials for OLEDs show significant parallel orientation with respect to the layers, which leads to strong anisotropy in their complex refractive index and electrical properties. Historically, anisotropy was not systematically taken into account in the optical design of OLEDs because the anisotropy was deemed very small. Although some papers include the anisotropy of the refractive index in optical simulations for OLEDs [11,12], the effects of the anisotropy of the refractive index on outcoupling have never been fully discussed. Previous papers consider only one specific stack and do not reflect on what kinds of anisotropy would be beneficial in certain layers. We now know that there are many OLED materials (mostly having linear, oblong or disk-like molecular shapes) that show strong anisotropy. Typically these organic layers are uniaxial with the c-axis perpendicular to the substrate [9]. Some organic molecules that exhibit strong anisotropy when thermally evaporated onto a substrate are shown in Fig. 2.

#241444 Received 21 May 2015; revised 3 Jul 2015; accepted 17 Jul 2015; published 4 Aug 2015

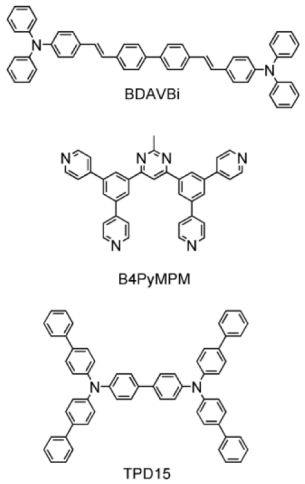

Fig. 2. Examples of small-molecule OLED materials exhibiting strong anisotropy when evaporated. (1) BDAVBi [4,4'-bis[4-(diphenylamino)styryl]biphenyl] [13] used as an emitting material, (2) B4PyMPM [4,6-Bis(3,5-di(pyridin-4-yl)phenyl)-2-methylpyrimidine] [14] used as an electron transport material, (3) TPD15 [N,N,N',N'-tetrakis(biphenyl-4-yl)benzidine] [10] used as a hole transport material.

In this article, the effect of anisotropy on optical outcoupling is investigated and a number of guidelines for the optical design based on anisotropic layers are put forth. Additionally, these findings can be used as guidelines for the development of new organics with superior optical properties. Important to note is that we investigate the anisotropy in the refractive index, i.e. birefringence, and the focus is not on oriented emitters. The topic of anisotropic emitters is now a very popular one [9,15] (as the orientation of the emitters determines the direction of the emission), yet it is our aim to investigate the effect of anisotropic refractive indices of charge transport materials. We will focus on anisotropy in the ETL and HTL layers (see Fig. 3) since the EML is usually much thinner and will have a much smaller impact. The analysis is performed in different steps. In section 2, the emission in the vertical direction (i.e. along the normal of the layers, away from the aluminum layer) is investigated. In section 3, the effect of the extra-ordinary refractive index n_e on the angle dependency of the dipole emission is investigated and in the fourth section, these two effects are combined and the overall effect on outcoupling efficiency is explored. The simulation method is based on the radiation of dipole antennas inside a one-dimensional microcavity combined with the scattering matrix method and is detailed elsewhere [16]. Throughout the remainder of this text, the same symbols and conventions will be used as in the work of Penninck et al. [16]. The dipole moment of the emitting dipoles is normalized such that they radiate 1 W in vacuum. The wavelength under investigation is chosen to coincide with the peak wavelength of photopic vision, 555 nm. The emitter is always considered to be infinitely thin and located in the middle of the emitting layer.

2. Vertical emission

In this section, the effect of the refractive index on the vertical emission is studied. This direction corresponds to the c-axis of the media and therefore only the ordinary refractive indices n_o of the media are relevant. The used stack is shown in Fig. 3 and values for the thicknesses and refractive indices can be found in Table 1.

#241444 Received 21 May 2015; revised 3 Jul 2015; accepted 17 Jul 2015; published 4 Aug 2015

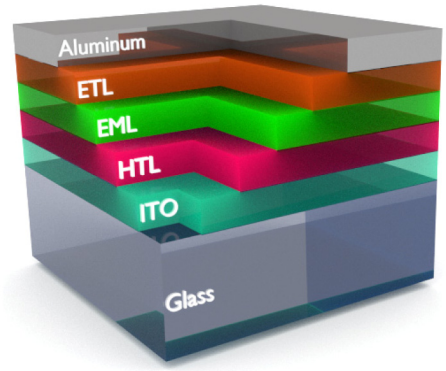

Fig. 3. Schematic drawing of the OLED stack used in the simulations. The stack consists of an aluminum layer, an electron transport layer (ETL), an emissive layer (EML), a hole transport layer (HTL), an indium tin oxide layer (ITO) and a glass substrate. Layer thicknesses are not to scale.

Table 1. Parameters for layers in the OLED stack used in simulations to investigate the emission in the vertical direction.

Material	Thickness	n_o
Aluminum	100 nm	1 + 6 j
ETL	10-150 nm	1.3 … 2.1
EML	10 nm	1.7
HTL	10-150 nm	1.3 … 2.1
ITO	77 nm	1.8
Glass	optically thick	1.5

Aluminum with a typical thickness of 100 nm is chosen for the reflective cathode. The value for n_o is varied for both the ETL and the HTL, while the refractive index for the EML remains fixed at 1.7 (isotropic), as it has little effect due to its small thickness. The ITO layer has a typical refractive index of 1.8. The optical thickness of the ITO is chosen to be a quarter wavelength (555 nm/(4·1.8) = 77 nm) because this maximizes the reflectivity for light traveling from the HTL to glass and leads to a maximum in the emission in the vertical direction, in the case where the refractive index of the HTL is below 1.8. Lastly, glass is used as the material of the substrate, a typical choice for OLEDs. All of these values are chosen such that they reflect a typical OLED device in an effort to ensure general applicability. In the simulations the value of n_o of the ETL and HTL is varied over a broad range, from 1.3 to 2.1. For each set of values, the optimal thickness of the layers is determined. This is necessary because there are interference effects at play in the vertical direction which are influenced by both the thicknesses and the refractive indices. To find the optimal vertical emission for each set of refractive indices, the thicknesses of the ETL and HTL are varied between 10 and 150 nm. The goal function in the optimization is the amplitude of the Poynting vector into the substrate perpendicular to the substrate interface. Note that in this document we limit ourselves to the so-called first maximum, the local optimum with the thinnest ETL and HTL layer. The result of these simulations are shown in Fig. 4. The figure represents the outcoupling efficiency, relative to the case with the refractive index of all organics set to n_o = 1.7. A strong dependency on n_o of the HTL and a weak dependency on the n_o of the ETL is observed. Looking back at the stack, it is easy to understand the reason why there is such a strong dependency on the n_o of the HTL: this value determines the reflectivity at the interface between the organics and the bottom two layers of the stack, ITO and the glass substrate. On the other hand, only a weak dependency on the n_o of the ETL is observed because the reflection at this side is dominated by the optical characteristics of the

#241444 Received 21 May 2015; revised 3 Jul 2015; accepted 17 Jul 2015; published 4 Aug 2015

reflective cathode and the interference effect is optimized for each value of n_o by selecting the optimal thickness. From Fig. 4 it is clear that the outcoupling efficiency in the vertical direction can be increased by about 30% if n_o of the HTL is reduced to 1.5. On the other hand, increasing n_o to 2.1 leads to a drop of more than 30%.

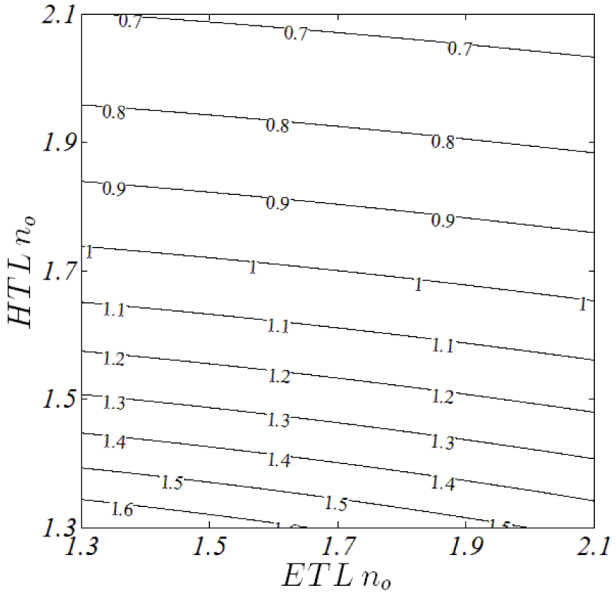

Fig. 4. Relative value (with respect to the case where both refractive indices are 1.7) of the outcoupling efficiency in the vertical direction as a function of n_o of the ETL and HTL.

3. Effect of changing n_e

In this section, the effect of changing the extra-ordinary refractive indices is investigated. The goal function is the fraction of the total radiation that is emitted into the substrate, henceforth called the outcoupling efficiency. Note that we consider the outcoupling efficiency for emission into the substrate. By doing this the reader can consider their extraction method of choice in order to minimize the amount of light trapped in substrate modes. This enables us to assess the true gain associated with the anisotropic layers. In order to limit the calculation time, the layer thicknesses are optimized for the isotropic case ($n_e = n_o = 1.7$ for all organic materials) and the resulting thicknesses are then used for the calculations with other values of n_e. This approach is motivated by the fact that interference effects have the largest impact for emission angles near the vertical direction, where only the (fixed) ordinary refractive index plays a role.

Table 2. Parameters for the layers used in the OLED stack to investigate the effect of changing n_e on the extraction efficiency.

Material	Thickness	n_o	n_e
Aluminum	100 nm	1 + 6 j	1 + 6 j
ETL	101 nm (optimized)	1.7	1.3 … 2.1
EML	10 nm	1.7	1.7
HTL	150 nm (optimized)	1.7	1.3 … 2.1
ITO	77 nm	1.8	1.8
Glass	optically thick	1.5	1.5

In the first step the optimization of the layer thicknesses was performed for $n_e = n_o = 1.7$. With the refractive indices given in Table 2, the local optimum, referred to as the so-called first maximum, disappears (i.e. is no longer an local optimum). We therefore decided to select the combination of layer thicknesses which resulted in the best outcoupling efficiency

#241444 Received 21 May 2015; revised 3 Jul 2015; accepted 17 Jul 2015; published 4 Aug 2015

within a limited parameter space (namely: 10-150 nm for both the ETL and HTL layer). The result is that the optimal layer thickness (using the outcoupling efficiency for random emitters as goal function) is 101 nm for the ETL layer and 150 nm for the HTL layer. In the second step the extra-ordinary refractive index n_e of both the ETL and HTL is varied between 1.3 and 2.1 and the integrated emission in glass of electrical dipoles in the EML is calculated. This is done for different dipole orientations in order get a complete overview. We consider three dipole orientations: the first is perpendicular to the interfaces, while the other two are mutually orthogonal ones, parallel to the interfaces. The latter two emissions are averaged and represent the emission for the parallel orientation. Considering the rotational symmetry of the problem, these form a complete set and the emission for randomly oriented dipoles can be found by averaging with weights 2/3 and 1/3 for the parallel and perpendicular orientation respectively. The simulated outcoupling efficiency for perpendicular, parallel and random emitters are shown in Fig. 5-7, respectively.

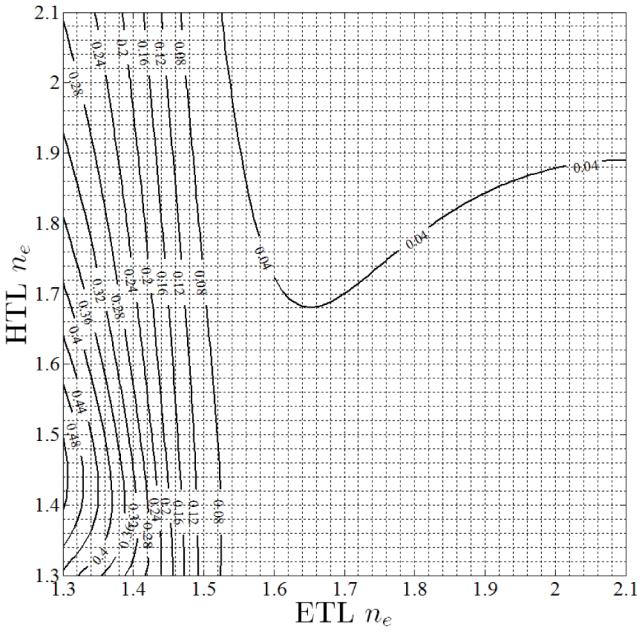

Fig. 5. Simulated outcoupling efficiency to glass for perpendicular dipoles. Calculations are made for the points on the grid, the contour lines are based on interpolation.

#241444 Received 21 May 2015; revised 3 Jul 2015; accepted 17 Jul 2015; published 4 Aug 2015

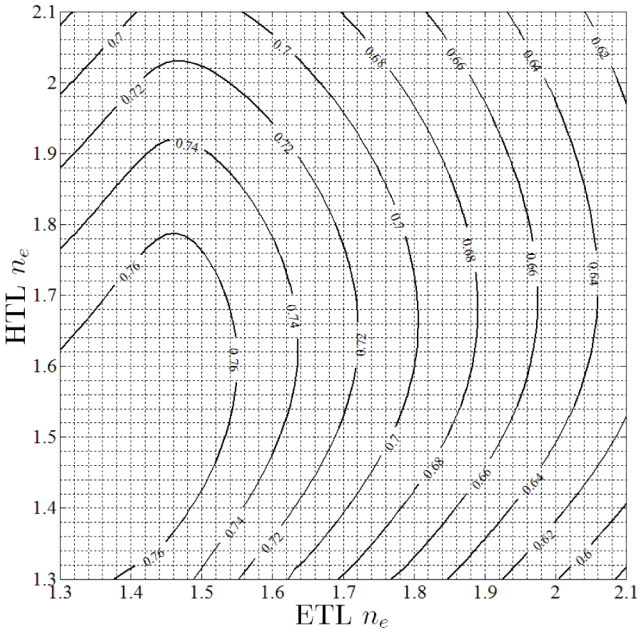

Fig. 6. Simulated outcoupling efficiency to glass for parallel dipoles. Calculations are made for the points on the grid, the contour lines are based on interpolation.

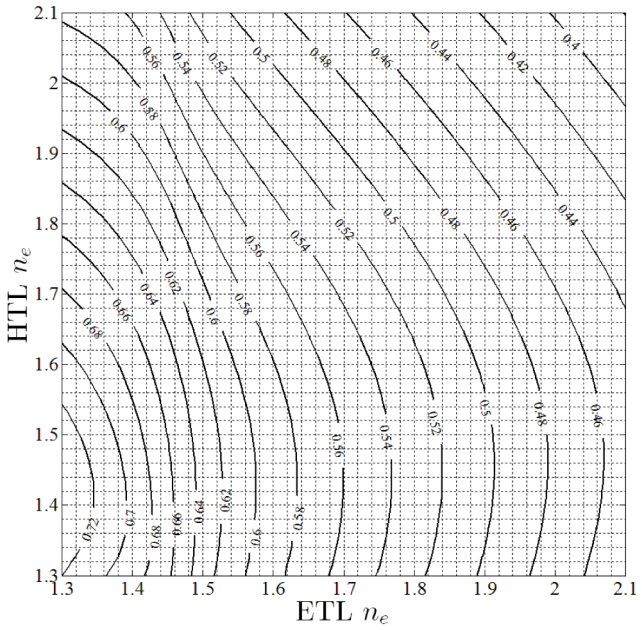

Fig. 7. Simulated outcoupling efficiency to glass for randomly oriented dipoles. Calculations are made for the points on the grid, the contour lines are based on interpolation.

Because most contour lines are more or less parallel to the y-axis, it is clear that changing the n_e of the ETL has the biggest impact on the outcoupling efficiency. Reducing the n_e of the ETL increases the outcoupling efficiency in most situations. For the HTL the outcoupling efficiency depends only weakly on n_e, for the perpendicular dipoles. When the emitters are

#241444 Received 21 May 2015; revised 3 Jul 2015; accepted 17 Jul 2015; published 4 Aug 2015

parallel, a fairly strong dependency on the HTL n_e is observed which results in a fairly strong dependency on the HTL n_e for random emitters.

In order to better understand these results it is interesting to investigate the emission of the dipoles in k-space. The emission distribution for different orientations of dipoles and different values of n_e are shown in Fig. 8-13.

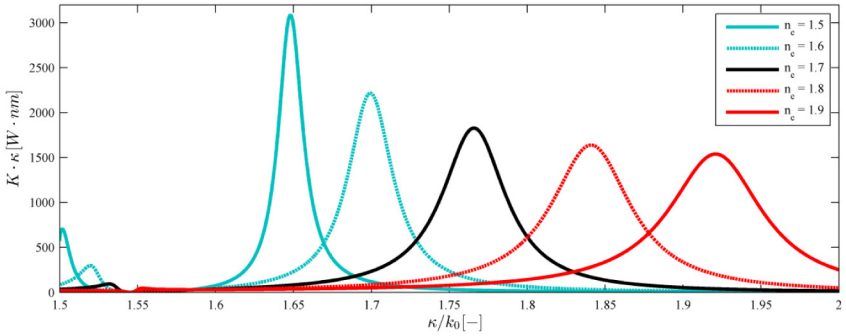

Fig. 8. Emission distribution for different ETL n_e with perpendicular dipole orientation. K is the power flux per unit κ^2 in the + z and -z directions in the plane of the emitter and κ designates the component of the wavevector parallel to the interfaces.

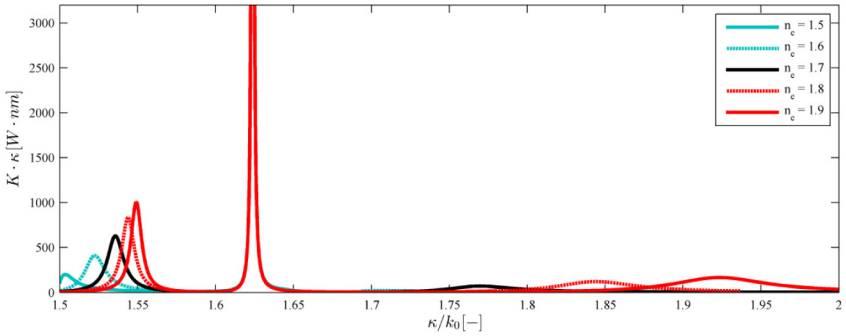

Fig. 9. Emission distribution for different ETL n_e with parallel dipole orientation. K is the power flux per unit κ^2 in the + z and -z directions in the plane of the emitter and κ designates the component of the wavevector parallel to the interfaces. The peak around $\kappa/k_0 = 1.62$ is not influenced by changes in n_e since it is a TE peak.

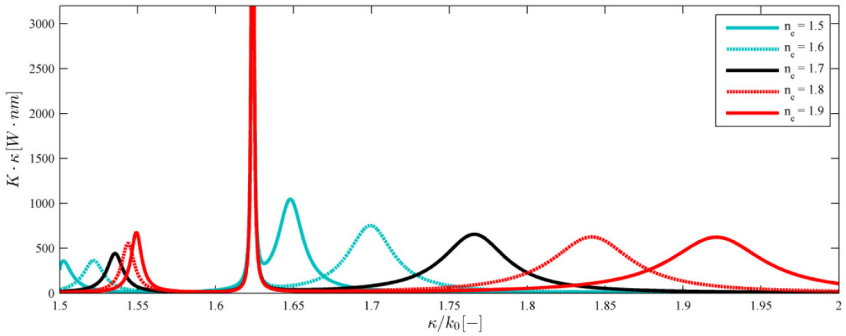

Fig. 10. Emission distribution for different ETL n_e with random dipole orientation. K is the power flux per unit κ^2 in the + z and -z directions in the plane of the emitter and κ designates the component of the wavevector parallel to the interfaces. The peak around $\kappa/k_0 = 1.62$ is not influenced by changes in n_e since it is a TE peak.

#241444 Received 21 May 2015; revised 3 Jul 2015; accepted 17 Jul 2015; published 4 Aug 2015

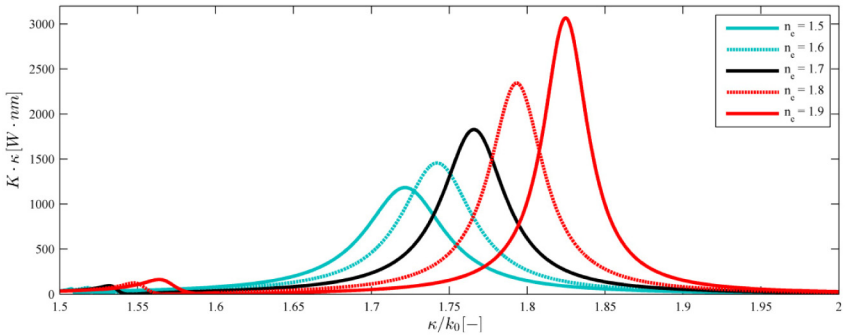

Fig. 11. Emission distribution for different HTL n_e with perpendicular dipole orientation. K is the power flux per unit κ^2 in the + z and -z directions in the plane of the emitter and κ designates the component of the wavevector parallel to the interfaces.

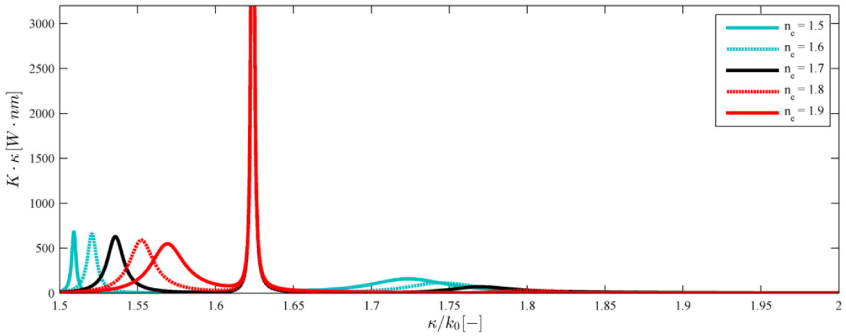

Fig. 12. Emission distribution for different HTL n_e with parallel dipole orientation. K is the power flux per unit κ^2 in the + z and -z directions in the plane of the emitter and κ designates the component of the wavevector parallel to the interfaces. The peak around $\kappa/k_0 = 1.62$ is not influenced by changes in n_e since it is a TE peak.

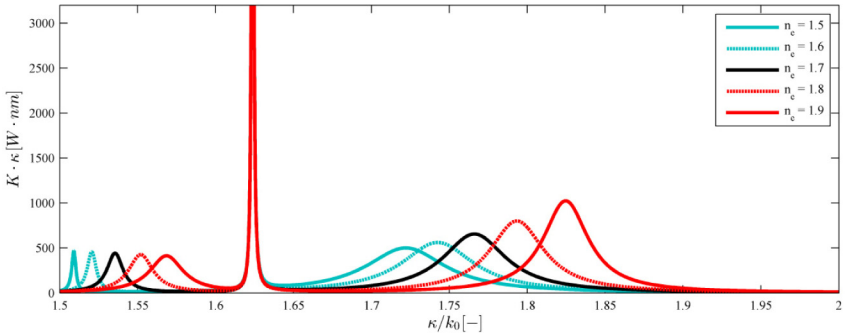

Fig. 13. Emission distribution for different HTL n_e with random dipole orientation. K is the power flux per unit κ^2 in the + z and -z directions in the plane of the emitter and κ designates the component of the wavevector parallel to the interfaces. The peak around $\kappa/k_0 = 1.62$ is not influenced by changes in n_e since it is a TE peak.

The figures above are constructed in such a way that the surface area under the curve scales with the total emitted power for the corresponding interval of κ. Changing the value of n_e only has significant influence on the emission for values of κ/k_0 greater than 1.5, which is why values lower than 1.5 are not shown. Note that the peak around $\kappa/k_0 = 1.62$ is not influenced by changing n_e because this peak is TE polarized and consequently only feels n_o.

#241444 Received 21 May 2015; revised 3 Jul 2015; accepted 17 Jul 2015; published 4 Aug 2015

Emission with κ/k_0 greater than 1.5 cannot propagate in the glass substrate and is thus trapped inside the organic stack and eventually absorbed. Using this observation we define $P_{trapped}$, P_{total} and the trapped fraction as

$$P_{trapped}[W] = \iint_{\kappa>1.5\cdot k_0}^{+\infty} K\, d\kappa^2 = \int_0^{2\pi} d\varphi \int_{1.5\cdot k_0}^{+\infty} K\cdot\kappa\, d\kappa = 2\pi \int_{1.5\cdot k_0}^{+\infty} K\cdot\kappa\, d\kappa, \quad (1)$$

$$P_{total}[W] = \iint_{0}^{+\infty} K\, d\kappa^2 = \int_0^{2\pi} d\varphi \int_{0}^{+\infty} K\cdot\kappa\, d\kappa = 2\pi \int_{0}^{+\infty} K\cdot\kappa\, d\kappa, \quad (2)$$

$$\text{Trapped Fraction}\ [\,\%\,] = \frac{P_{trapped}}{P_{total}}, \quad (3)$$

with K the power flux per unit κ^2 in the + z and -z directions in the plane of the emitter. In Fig. 14 the trapped fraction is shown for the three different dipole orientations, while the values for n_e of the HTL and ETL are varied between 1.3 and 2.1. This figure gives insight into how the radiation pattern of the dipoles change under the influence of changing n_e. For the ETL we observe that lowering the value of n_e will always be accompanied by a drop in radiation emitted into these trapped directions. The effect is strongest for perpendicular emitters, which is to be expected, since perpendicular emitters emit a larger portion of their total emission into trapped directions. For the parallel and random oriented emitters we observe the same trend and we can conclude that low values of ETL n_e are effective at lowering the trapped fraction. For the HTL the effect is more intricate and less pronounced for this combination of layers. In Fig. 15 we show the same graph for a stack where the ETL is 54 nm thick and the HTL 115 nm. This stack has a very similar outcoupling efficiency (53% for random emitter orientation) but was not selected as the optimum since it is not a local optimum. A slightly higher value (53.8% for random emitter orientation) is achievable with the stack detailed in Table 2 (which was selected because it gave the maximum outcoupling efficiency within the limits of the parameter space). This stack (54 nm ETL and 115 nm HTL) is relevant since it still results in high outcoupling efficiencies and corresponds to the location in the parameter space where the local optimum would be found with slightly different refractive indices. The difficulty in this is that the so-called first maximum is not a local optimum for this particular combination of layers (there is a slow monotonous increase between the so-called first and second maximum). This stack is of interest since it illustrates the effect of changing the ETL n_e and HTL n_e more clearly. Lowering the value of HTL n_e results in a decrease in the trapped fraction for perpendicular emitters whereas it results in an increase in the trapped fraction for parallel emitters. Consequently the effect on random emitters is almost non-existent. From the optical viewpoint, we can say that HTL materials with high values for n_e should be used for high outcoupling in a device that utilizes the superior parallel emitters. However, it should also be mentioned that a high n_e requires perpendicular orientation of charge transport materials and may have a negative effect on the charge transport in the vertical direction [9].

#241444 Received 21 May 2015; revised 3 Jul 2015; accepted 17 Jul 2015; published 4 Aug 2015

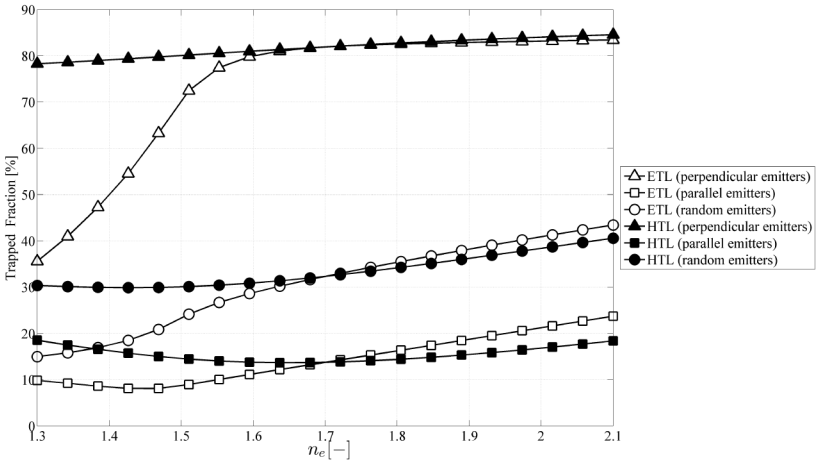

Fig. 14. Integrated emission for κ/k_0 larger than 1.5 for different orientations of the dipoles and for different values of n_e for the ETL and HTL layers. One value of n_e is fixed to 1.7, the other one (ETL or HTL, see legend) is varied between 1.3 and 2.1. The stack corresponds to the stack detailed in Table 2.

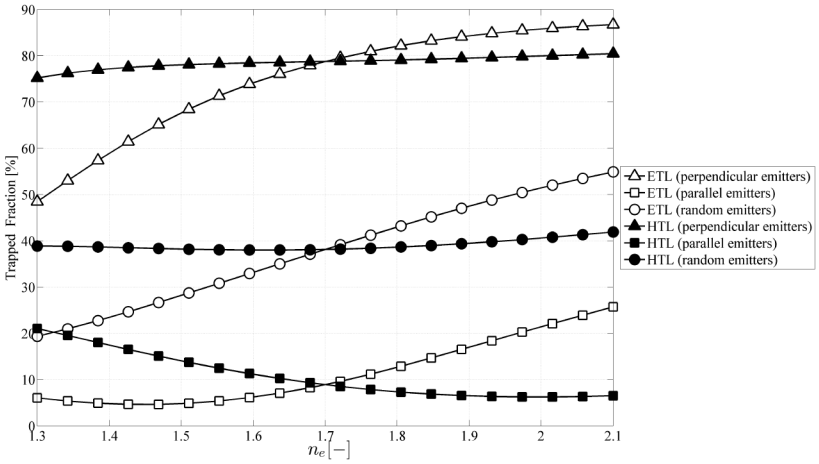

Fig. 15. Integrated emission for κ/k_0 larger than 1.5 for different orientations of the dipoles and for different values of n_e for the ETL and HTL layers. One value of n_e is fixed to 1.7, the other one (ETL or HTL, see legend) is varied between 1.3 and 2.1. The stack is similar to the stack detailed in Table 2 but has an ETL thickness of 54 nm and a HTL thickness of 115 nm.

In this section, we have shown that n_e can have a significant influence on the fraction of the light that is coupled to trapped directions and eventually lost through absorption. For the ETL it is clear that losses can be lowered by reducing the value of n_e. The reason for this is that the plasmonic loss peak in the emission spectrum becomes increasingly narrow for smaller n_e values. The loss associated with the perpendicular dipoles is reduced most significantly, since they couple more strongly to the plasmonic modes. For the HTL it depends on the dipole orientation. With parallel emitters benefiting from high values of n_e and perpendicular emitters from low values. Looking back at the previous section we remember that lowering n_o of the HTL will have a positive effect on the vertical emission. In an optimal device, from a purely optical viewpoint, we would thus prefer parallel emitters with a HTL with high n_e and low n_o. These opposing requirements for n_e and n_o are a

#241444 Received 21 May 2015; revised 3 Jul 2015; accepted 17 Jul 2015; published 4 Aug 2015

testament to the advantage of using anisotropic materials over isotropic materials in the optical design of OLEDs.

4. Effect of anisotropy on OLED emission

In real materials n_e and n_o are given and both aforementioned effects play a role when different materials are compared. Now we can investigate the combined effect of varying the refractive indices in the ETL and HTL. In this section, we focus on the effect of the anisotropy Δn, while keeping the isotropic (averaged) refractive index n_{iso} constant. These values are defined as:

$$\Delta n = n_e - n_o \,,\; n_{iso} = \left[\frac{2n_o^2 + n_e^2}{3} \right]^{1/2} . \tag{4}$$

By keeping the isotropic refractive index of the materials constant (n_{iso} = 1.7) we avoid including the study of the refractive index of isotropic materials, which is not the aim of this paper. A grid of nine sets (see Fig. 16) of refractive indices is used, with three values for Δn_{ETL} and three values for Δn_{HTL}. These values for Δn are comparable to values found in literature [16]. It has been shown that even though most amorphous organic semiconductor films have negative anisotropy, when thermally evaporated on a substrate, they can be made to show positive anisotropy if they are deposited on a heated substrate [9,10]. For each configuration, the thicknesses of the ETL and HTL layers are optimized to obtain the local optimum (i.e. the so-called first maximum). By optimizing the thicknesses for each configuration, we ensure that the obtained outcoupling efficiency is the highest possible value, corresponding to the structure with optimized interference effects (values can be found in Appendix A). In some cases the so-called first maximum is no longer a local optimum. In this case we chose the highest value within the parameter sweep of 10 to 150 nm. The sweep was also done for a larger parameter space where the absolute maximum was evaluated. These results are optically interesting but are not limited to the so-called first maximum (they often correspond to the second maximum). They can be found in Appendix B.

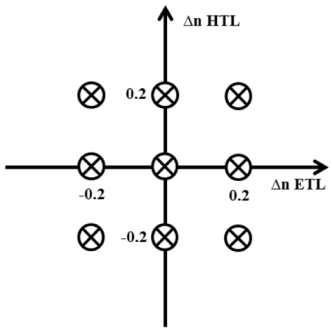

Fig. 16. Grid of investigated points.

In this section we carry out detailed calculations taking into account the full angle dependency, polarization and interference effects for the 9 given sets of anisotropy (see Fig. 16). In addition, the results for different orientations of the emitting dipoles are analyzed. We investigate both parallel and perpendicular dipoles. From these, the emission in the case of random dipoles can be determined. From the simulations, the outcoupling efficiency η_{out} can be determined as

#241444 Received 21 May 2015; revised 3 Jul 2015; accepted 17 Jul 2015; published 4 Aug 2015

$$\eta_{out} = \frac{\int_0^{\infty} K_{sub}\, d\kappa^2}{\int_0^{\infty} K_{EML}\, d\kappa^2} \tag{5}$$

where K_{sub} and K_{EML} are respectively the power flux per unit κ^2 into the substrate (only in the + z direction) and the total power emitted by the emitter (in both the + z and -z directions). This outcoupling efficiency is optimized for each set of refractive indices, by varying the thickness of the ETL and HTL. F, the Purcell enhancement factor related to the optical-environment [17], is calculated as

$$\mathrm{F} = \frac{\int_0^{\infty} K_{EML}\, d\kappa^2}{\int_0^{\infty} K_{inf}\, d\kappa^2}, \tag{6}$$

where K_{inf} is the total power flux per unit κ^2 of a dipole (in both the + z and -z directions) when it is located in an infinite medium with the optical characteristics of the EML ($n_e = n_o = 1.7$). From the value of F and the decay characteristics of specific emitters in a thick EML layer, the radiative efficiency of the dipole in the specific stack can be determined as follows:

$$\eta_{rad} = \frac{F \cdot \Gamma_{r,0}}{F \cdot \Gamma_{r,0} + \Gamma_{nr}}, \tag{7}$$

where $\Gamma_{r,0}$ is the radiative fraction of the decay rate in an infinite EML medium and Γ_{nr} is the non-radiative fraction of the decay rate in an infinite EML medium, with $\Gamma_{r,0} + \Gamma_{nr} = 1$. From the outcoupling efficiency η_{out} and the radiative efficiency η_{rad} the external quantum efficiency (EQE) is calculated as follows;

$$EQE_{sub} = \frac{N_{ph,sub}}{N_{h^+}} = \eta_{cb}\eta_{st}\eta_{rad}\eta_{out}, \tag{8}$$

with $N_{ph,sub}$ the number of photons reaching the substrate, N_h^+ the number of injection holes, η_{cb} the charge balance efficiency (assumed to be unity) and η_{st} the singlet/triplet efficiency (0.25 for fluorescent emitters and unity for phosphorescent emitters). As long as the fraction of non-radiative decay is negligible ($\Gamma_{nr} \ll 1$), F does not play a role for the EQE_{sub}. However, when Γ_{nr} is large, it is beneficial to have a higher value for F to increase the EQE [8]. In what follows the values of F will be given but no assumptions will be made concerning Γ_{nr}. This way the reader can determine EQE_{sub} values for a specific type of emitter. Note that EQE_{sub} is identical to η_{out} in case a phosphorescent emitter with 100% efficiency is used with perfect charge balance.

4.1 Parallel emitter orientation

When the dipoles are oriented parallel to the layers, we expect a good outcoupling because the emission is mainly within the extraction cone [15]. In Figs. 17 and 18, the structures have been optimized for parallel dipoles using the outcoupling efficiency as a goal function. The optimized layer thicknesses can be found in Appendix A in Table 3.

#241444 Received 21 May 2015; revised 3 Jul 2015; accepted 17 Jul 2015; published 4 Aug 2015

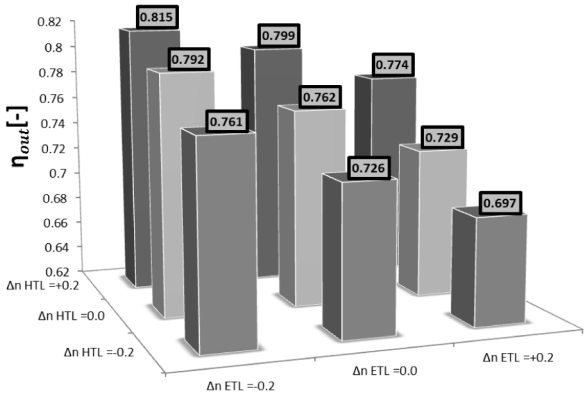

Fig. 17. Maximum outcoupling efficiency for different anisotropic situations in the case of parallel emitters. For every combination the interference effects are optimized by adjusting the ETL and HTL layer thicknesses.

The corresponding values for F are given below.

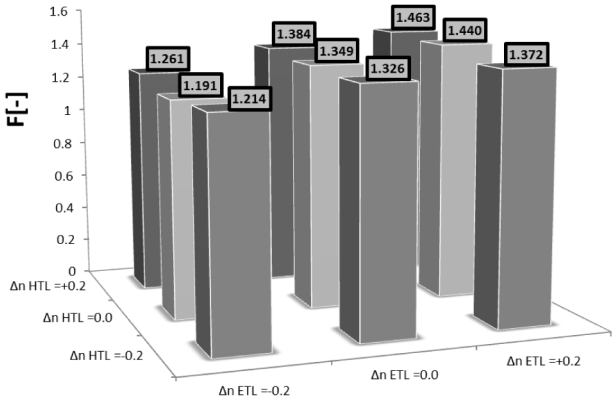

Fig. 18. Values of F corresponding to the optimized stacks shown in the previous figure. These are the F values for the anisotropic stacks with optimized interference effects in the case of parallel emitters.

From Fig. 17 we find that, for parallel dipoles, a good choice of anisotropic materials gives a 7% increase in maximum outcoupling efficiency whereas a poor choice corresponds with a 8.4% decrease. Overall we can say that the correct or poor selection of anisotropic materials can account for a 15.4% change in maximum outcoupling efficiency. For the ETL we find that negatively anisotropic layers give the best result, which corresponds to our observation that n_e needs to be as small as possible (see Fig. 14 and 15). Combining this with the weak influence of n_o, (see Fig. 4) we conclude that negatively anisotropic layers are optimal for the ETL. For the HTL layer we expect from Fig. 4, 14 and 15 to find that positive anisotropy will boost outcoupling efficiency, as this can accommodate a low n_o and a high n_e. These opposing requirements for n_o and n_e confirm the superiority of anisotropic layers over isotropic ones. For the F values we observe opposing trends which can be attributed to the fact that an increased coupling to plasmonic modes will increase the total emission of the dipole and thus the value for F. For emitters with high Γ_{nr} a higher value of F helps to increase the EQE_{sub} although this will have little impact on highly efficient emitters ($\Gamma_{nr} \ll 1$).

#241444 Received 21 May 2015; revised 3 Jul 2015; accepted 17 Jul 2015; published 4 Aug 2015

4.2 Perpendicular emitter orientation

When dipoles are oriented perpendicular to the layers we expect significantly smaller values for the outcoupling efficiency. In Figs. 19 and 20, the structures have been optimized, for perpendicular dipoles, using the outcoupling efficiency as a goal function. For perpendicular dipoles, we increase the parameter space (raising the maximum thickness to 500 nm for both the transport layers), since the maxima are usually found for relatively large values of the ETL and HTL. The optimized layer thicknesses can be found in Appendix A in Table 4. These layers are rather thick but can be accommodated using appropriate doping to increase charge mobility [18]. The reader might find the outcoupling efficiencies to be significantly larger than one would normally expect for perpendicular emitters. These high values are a result of the large parameter space, which contains thick ETL and HTL layers. We have to use these thick layers in order to find clear maxima to quantify the optical effects.

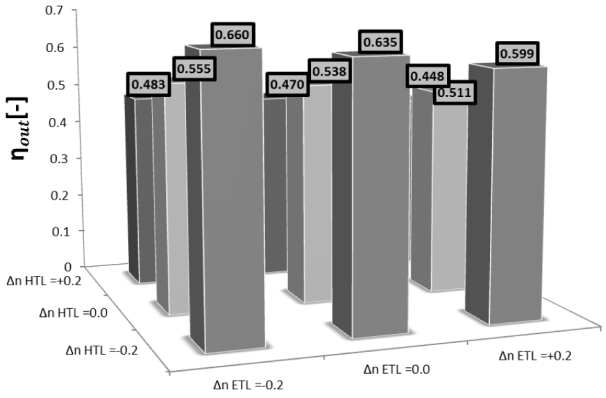

Fig. 19. Maximum outcoupling efficiency for different anisotropic situations in the case of perpendicular emitters. For every combination the interference effects are optimized by adjusting the ETL and HTL layer thicknesses.

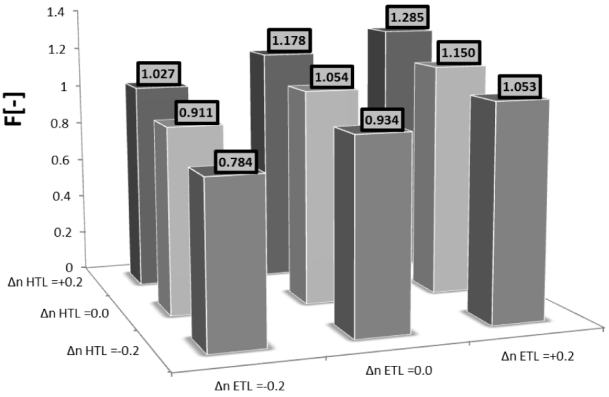

Fig. 20. Values of F corresponding to the optimized stacks from the previous figure. These are the F values for the anisotropic stacks with optimized interference effects in the case of perpendicular emitters.

From the figures above we find that, for perpendicular dipoles, a good choice of anisotropic materials gives a 22.7% increase in maximum outcoupling efficiency whereas a poor choice corresponds with a 16.7% decrease. Overall we can say that the correct or poor selection of anisotropic materials can account for a 39.4% change in maximum outcoupling efficiency. For the ETL the conclusions are the same as for parallel dipoles, being that negatively anisotropic materials give the best results. For the HTL however, the conclusions

#241444 Received 21 May 2015; revised 3 Jul 2015; accepted 17 Jul 2015; published 4 Aug 2015

are opposing to the case of parallel emitters, where a positively anisotropic material resulted in better outcoupling. This can be understood if we look at Fig. 14 and 15 where we see that, in the case of perpendicular emitters, low values of n_e are superior. This observation combined with the knowledge that perpendicular emitters do not emit in the perpendicular direction enables us to understand why negatively anisotropic layers give the best results for perpendicular emitters.

4.3 Random emitter orientation

In Figs. 21 and 22 the structures have been optimized, for randomly oriented dipoles, using the outcoupling efficiency as a goal function. Note that in the two previous sections the outcoupling efficiency was optimized for the parallel and perpendicular dipoles separately. The optimal thicknesses found for these two situations differ strongly and the thicknesses giving the optimal outcoupling for randomly oriented dipoles will differ again. The values that we find for randomly oriented dipoles are thus not simply an average of the two previous situations. The optimized thicknesses can be found in Appendix A in Table 5.

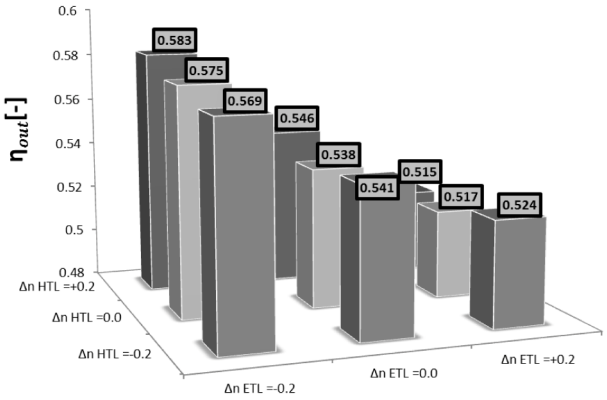

Fig. 21. Maximum outcoupling efficiency for different anisotropic situations in the case of random emitters. For every combination the interference effects are optimized by adjusting the ETL and HTL layer thicknesses.

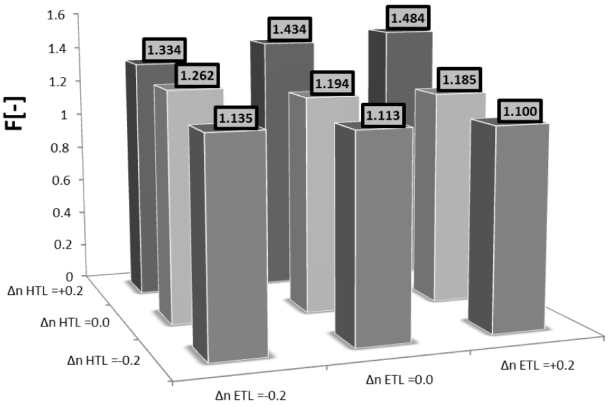

Fig. 22. Values of F corresponding to the optimized stacks from the previous figure. These are the F values for the anisotropic stacks with optimized interference effects in the case of random emitters.

From the figures above we find that, for randomly oriented dipoles, a good choice of anisotropic materials gives a 8.4% increase in maximum outcoupling efficiency whereas a poor choice corresponds with a 4.3% decrease. Overall we can say that the correct or poor

#241444 Received 21 May 2015; revised 3 Jul 2015; accepted 17 Jul 2015; published 4 Aug 2015

selection of anisotropic materials can account for a 12.7% change in maximum outcoupling efficiency. For randomly oriented emitters, we observe a very strong dependency on the ETL anisotropy, with negatively anisotropic materials giving the best results. This corresponds to the conclusion for the perpendicular and parallel orientations. For the HTL we observe a weaker dependency with positively anisotropic materials performing best. This can be explained by the competing effects for parallel and perpendicular dipoles. Due to the fact that the effect is stronger for parallel emitters and the fact that they contribute twice to the emission profile of a random emitter, the positively anisotropic HTL layer gives slightly superior performance.

4.4 Effect of spectral width of the emitter

Throughout this document a monochromatic source is assumed in order to simplify simulations. In reality, organic emitters have a rather broad emission spectrum which raises the question whether the conclusions in the above sections still hold for realistic emitters. To verify this, we take the results for parallel emitters from Appendix B and give the emitter an artificial spectrum. We assume a Gaussian emission with 555 nm as the central wavelength and vary the FWHM. We expect to see a drop in the overall efficiency for increasing FWHM, since the stack is optimized for the central wavelength. A realistic value for the FWHM for organic emitters is between 50 and 100 nm (AlQ3 has a FWHM of around 75 nm).

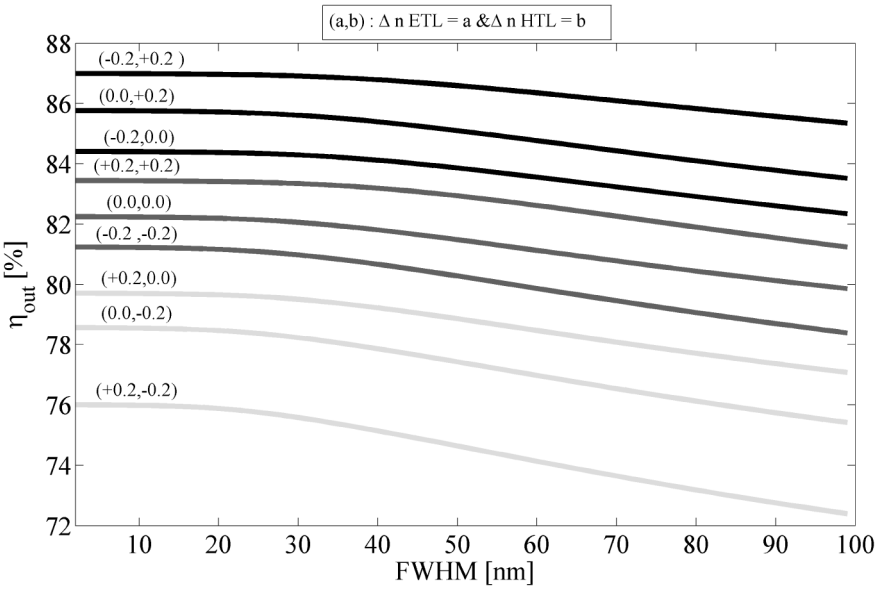

Fig. 23. Dependency of the outcoupling efficiency on the FWHM of the emission spectrum for materials with different anisotropies in refractive index (Δn_{ETL}, Δn_{HTL}). The 9 lines correspond to the stacks from Appendix B.

Figure 23 shows that all outcoupling efficiencies decrease with increasing FWHM, and that the characteristics do not cross. This means that using monochromatic emitters leads to a slight overestimation of the outcoupling efficiencies, but also that the dependency on the refractive index anisotropy remains valid, even for spectra with relatively high FWHM. For the parallel emitters we observe that the difference between the best and worst stacks increases with the FWHM of the emitters. This leads us to believe that we can expect slightly better improvement factors for realistic emitters.

#241444 Received 21 May 2015; revised 3 Jul 2015; accepted 17 Jul 2015; published 4 Aug 2015

5. Conclusions

We have studied the effect of anisotropy on the optical outcoupling of planar OLEDs. We first investigated the effect of changing n_o and the effect of changing n_e separately. We then combined the two effects by looking at realistic anisotropies. Throughout this analysis we investigated these effects for different dipole orientations, which proved to be a useful approach.

For parallel dipoles, we find that the HTL and ETL have opposing anisotropic requirements. The ETL layer increases outcoupling efficiency when negatively anisotropic, whereas negatively anisotropic HTL layers give a decrease in outcoupling efficiency. Important to note here is that parallel dipoles are an interesting case because they show higher outcoupling efficiencies in general, due to their emission pattern, and are consequently of interest for highly efficient OLEDs. From Fig. 17 we also conclude that a good choice of anisotropic materials gives a 7% increase in maximum outcoupling efficiency whereas a poor choice corresponds with a 8.4% decrease. Overall we can say that the correct or poor selection of anisotropic materials can account for a 15.4% change in maximum outcoupling efficiency for parallel emitters. For perpendicular dipoles the requirements are different than for parallel dipoles. Negative anisotropy is desirable for both the ETL and HTL layer. Important to note here is that the effect of the HTL layer is notably smaller than the effect of the ETL. The overall impact of a poor or correct choice of anisotropic materials can account for a 39.4% change in maximum outcoupling efficiency for perpendicular emitters. For random dipoles the effects are a combination of the perpendicular and parallel dipoles with a total impact of 12.7%.

In this study we proposed a number of guidelines for the design of OLEDs with anisotropic layers, in order to increase outcoupling efficiency. Depending on the emitter orientation these guidelines differ. In literature this has never been systematically investigated, to the best of our knowledge. In conclusion we can say that in order to create an OLED with high outcoupling efficiency, with respect to anisotropy, one should have a negatively anisotropic ETL layer, emitters that are parallel and a HTL with positive anisotropy.

Appendix A

Table 3. Optimized thicknesses for the OLEDs in Fig. 17 and 18 Parameter space limited to 10-150 nm for both ETL and HTL.

(ETL thickness, HTL thickness)	Δn ETL = –0.2	Δn ETL = 0.0	Δn ETL = + 0.2
Δn HTL = + 0.2	(58 nm, 135 nm)	(63 nm, 111 nm)	(68 nm, 97 nm)
Δn HTL = 0.0	(58 nm, 150 nm)	(64 nm, 111 nm)	(68 nm, 97 nm)
Δn HTL = –0.2	(63 nm, 150 nm)	(77 nm, 150 nm)	(92 nm, 150 nm)

Table 4. Optimized thicknesses for the OLEDs in Fig. 19 and 20. Parameter space limited to 10-500 nm for both ETL and HTL.

(ETL thickness, HTL thickness)	Δn ETL = –0.2	Δn ETL = 0.0	Δn ETL = + 0.2
Δn HTL = + 0.2	(230 nm, 246 nm)	(212 nm, 246 nm)	(195 nm, 246 nm)
Δn HTL = 0.0	(230 nm, 263 nm)	(212 nm, 263 nm)	(195 nm, 280 nm)
Δn HTL = –0.2	(246 nm, 364 nm)	(212 nm, 381 nm)	(212 nm, 364 nm)

#241444 Received 21 May 2015; revised 3 Jul 2015; accepted 17 Jul 2015; published 4 Aug 2015

Table 5. Optimized thicknesses for the OLEDs in Fig. 21 and 22. Parameter space limited to 10-150 nm for both ETL and HTL.

(ETL thickness, HTL thickness)	Δn ETL = –0.2	Δn ETL = 0.0	Δn ETL = + 0.2
Δn HTL = + 0.2	(78 nm, 116 nm)	(82 nm, 92 nm)	(92 nm, 77 nm)
Δn HTL = 0.0	(77 nm, 116 nm)	(101 nm, 150 nm)	(116 nm, 150 nm)
Δn HTL = –0.2	(87 nm, 150 nm)	(106 nm, 150 nm)	(121 nm, 150 nm)

Appendix B

A parameter sweep of 10-500 nm for both the ETL and HTL layer was used to find the absolute maximum outcoupling efficiency into the substrate. This was done for the parallel and random emitters. Even though some of these thicknesses (see Tables 6 and 7) require the use of dopants in realistic devices, these results allow for an absolute quantification of the benefit of anisotropic materials.

Parallel emitter orientation

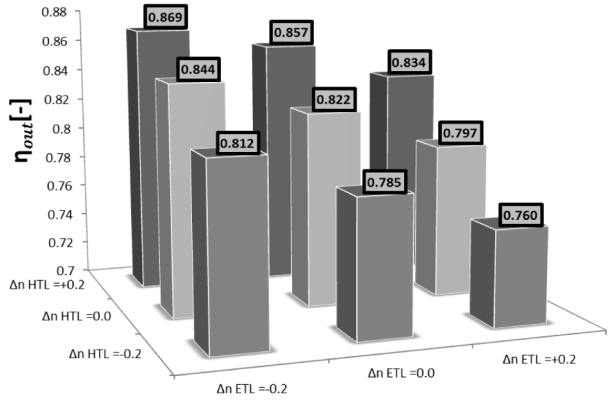

Fig. 24. Maximum outcoupling efficiency for different anisotropic situations in the case of parallel emitters. For every combination the interference effects are optimized by adjusting the ETL and HTL layer thicknesses over a large parameter space.

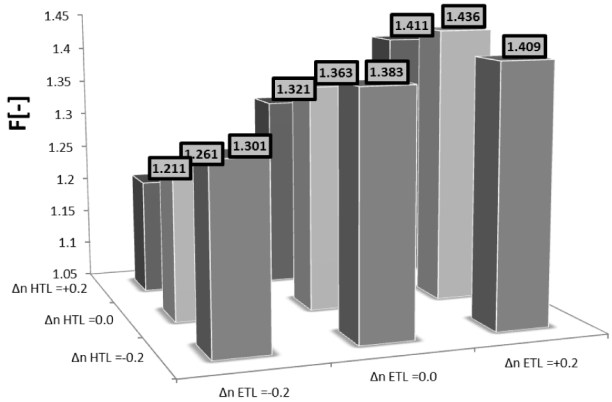

Fig. 25. Values of F corresponding to the optimized stacks shown in the previous figure. These are the F values for the anisotropic stacks with optimized interference effects in the case of parallel emitters.

#241444 Received 21 May 2015; revised 3 Jul 2015; accepted 17 Jul 2015; published 4 Aug 2015

Table 6. Optimized thicknesses for the OLEDs in Fig. 24 and 25. Parameter space limited to 10-500 nm for both ETL and HTL.

(ETL thickness, HTL thickness)	Δn ETL = –0.2	Δn ETL = 0.0	Δn ETL = + 0.2
Δn HTL = + 0.2	(63 nm, 365 nm)	(72 nm, 365 nm)	(84 nm, 351 nm)
Δn HTL = 0.0	(63 nm, 293 nm)	(72 nm, 293 nm)	(87 nm, 287 nm)
Δn HTL = –0.2	(68 nm, 253 nm)	(79 nm, 250 nm)	(96 nm, 246 nm)

Random emitter orientation

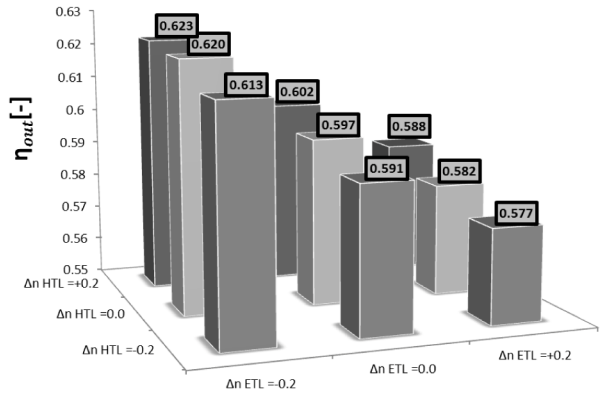

Fig. 26. Maximum outcoupling efficiency for different anisotropic situations in the case of random emitters. For every combination the interference effects are optimized by adjusting the ETL and HTL layer thicknesses over a large parameter space.

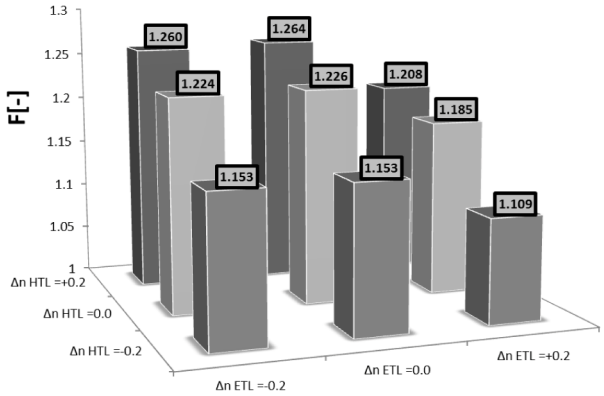

Fig. 27. Values of F corresponding to the optimized stacks shown in the previous figure. These are the F values for the anisotropic stacks with optimized interference effects in the case of parallel emitters.

Table 7. Optimized thicknesses for the OLEDs in Fig. 26 and 27. Parameter space limited to 10-500 nm for both ETL and HTL.

(ETL thickness, HTL thickness)	Δn ETL = –0.2	Δn ETL = 0.0	Δn ETL = + 0.2
Δn HTL = + 0.2	(87 nm, 310 nm)	(101 nm, 317 nm)	(121 nm, 317 nm)
Δn HTL = 0.0	(87 nm, 262 nm)	(101 nm, 256 nm)	(118 nm, 267 nm)
Δn HTL = –0.2	(90 nm, 232 nm)	(104 nm, 229 nm)	(122 nm, 233 nm)

Acknowledgments

The university of Ghent would like to thank the Belgian Agentschap voor innovatie door wetenschap en techniek (contract IWT 131498) and the Interuniversity Attraction Poles

#241444 Received 21 May 2015; revised 3 Jul 2015; accepted 17 Jul 2015; published 4 Aug 2015

program of the Belgian Science Policy Office (grant IAP P7-35 «photonics@be») for funding. D. Y. would like to thank KAKENHI (Grant Number 25708038) from Japan Society for the Promotion of Science (JSPS) for funding.

#241444 Received 21 May 2015; revised 3 Jul 2015; accepted 17 Jul 2015; published 4 Aug 2015